The 2009 IEEE/RSJ International Conference on
Intelligent Robots and Systems
October 11-15, 2009 St. Louis, USA

Motion Control of Passive Mobile Robot Consisting of Casters with Servo Brakes

Masao Saida, Yasuhisa Hirata and Kazuhiro Kosuge

Abstract— **In this paper, we introduce a passive mobile robot with casters developed based on the concept of passive robotics. This mobile robot consists of two casters with servo brakes, one passive rigid wheel and a controller. We can manipulate the robot by controlling external force/moment applied by a human based on the control of the servo brakes attached to the casters. We consider the characteristics of the servo brakes and control the brake torque of each caster based on the braking force and moment constraint so that several motion functions of the robot are realized based on the applied force. This allows the robot to track a path without using servo motors. The motion control based on the environment information is also realized, so that we could avoid the collision with obstacles. These functions are implemented to the robot experimentally and experimental results illustrate the validity of the robot system and its control method.**

I. Introduction

Most of robots have been used as industrial robots in factories to replace humans doing tasks, which humans do not want to do or could not do, and have been isolated from humans. In these days, however, we expect to utilize robot systems in many fields such as home, office and hospital in cooperation with humans. For practical use of the robot systems with physical interaction, we need to consider safety of their users. Most of the conventional intelligent robot systems have servo motors for controlling their motion. However, if we cannot appropriately control the servo motors of the intelligent systems, they move unintentionally and might be dangerous for humans.

On the other hand, from a safety point of view, Goswami et al. proposed the concept of passive robotics [1], in which a system moves passively based on external force and moment without using servo motors, and Peshkin et al. developed an object handling system called Cobot [2], in which its steering angle is only controlled by the servo motor.

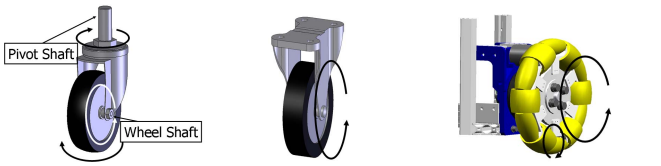

(a) Caster (b) Rigid Wheel (c) Omni-Directional Wheel

Fig. 1. Type of Wheel

M. Saida, Y. Hirata and K. Kosuge are with Derartment of Bioengineering and Robotics, Tohoku University, 6-6-01, Aoba, Aramaki, Aoba-ku, Sendai 980-8579, JAPAN {saida, hirata, kosuge}@irs.mech.tohoku.ac.jp

The concept of the passive robot has been extended to many fields. Wasson et al. [3] and Rentschler et al. [4] proposed passive intelligent walkers. These passive systems are intrinsically safe because they cannot move unintentionally with driving force. Thus, passive robotics will prove useful in many types of intelligent systems through physical interaction between the systems and humans.

We have also developed passive intelligent walker called RT Walker to support the walking of the handicapped people including the elderly [5]. It differs from other passive robots in that they control servo brakes appropriately to realize several functions without using any servo motors. We have extended the brake control technologies of the RT Walker to the control of the omni-directional object handling robot called PRP (Passive Robot Porter) [6].

In this research, we develop a new passive-type object handling robot system. First, we define the names of three kinds of wheels as shown in Fig. 1. In the conventional researches on our passive mobile robots including the RT Walker and the PRP, we have used rigid wheels or omni-directional wheels with servo brakes. In the living environment, however, we can transfer or handle many kinds of objects by using casters.

Here, we focus on casters. A caster has two rotary shafts: wheel shaft and pivot shaft. The pivot shaft is separately placed from the wheel shaft at the length of offset. Since the pivot shaft rotates passively based on external force/moment, the caster can move in all directions similar to an omni-directional wheel. Different from the omni-directional wheel, the caster has advantages such as moving with less vibration,

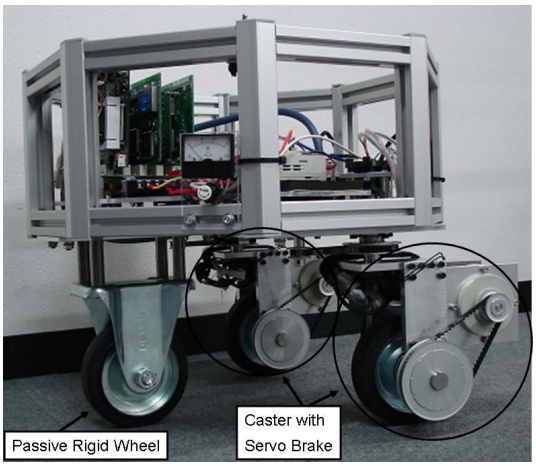

Fig. 2. Passive Mobile Robot Consisting of Casters with Servo Brakes

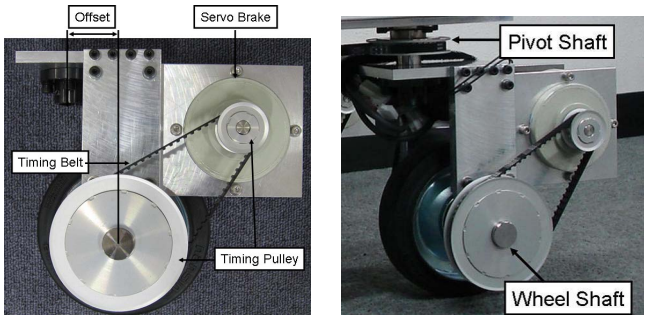

Fig. 3. Caster with Brake

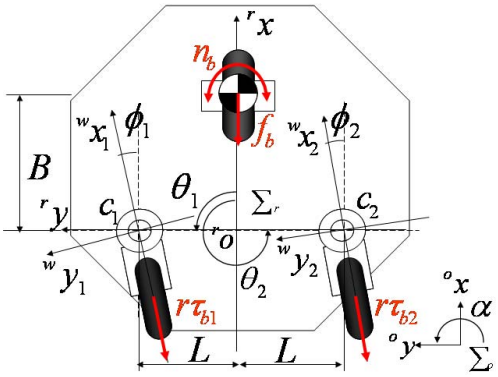

Fig. 4. Configuration of Robot

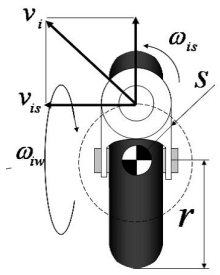

Fig. 5. Configuration of Caster

high withstand load, and high performance of climbing steps because a caster consists of a rigid wheel. Therefore, casters are widely used in order to move many kinds of objects in our daily lives.

However, the control of the system with casters is difficult because we have to control two rotary shafts (wheel shaft and pivot shaft) per one caster. Controlling the moving system with casters is challenging because of its complex structure. If we control the system with casters based on the concept of passive robotics, as well as achieving a high performance on object handling system, we could develop several kinds of passive-type moving bases depending on the applications and add the many functions such as collision avoidance, path tracking etc. to the moving bases which are wildly used in real world.

In this research, we develop a new passive-type mobile robot system consisting of casters with servo brakes. In this paper, firstly we introduce the robot consisting of two casters with servo brakes and one passive rigid wheel. Next, we propose a fundamental motion control algorithm of this robot system. In addition, we explain the braking force/moment constraint based on the characteristics of the servo brake and analyze the relationship between the direction of casters and the feasible braking force and moment. Finally, experimental results on the path tracking motion control and the collision avoidance motion control are shown to illustrate the validity of the proposed system and algorithm.

II. Passive Mobile Robot consisting of Casters

We develop a passive mobile robot with casters as shown in Fig. 2 based on the concept of the passive robotics [1]. The robot consists of two casters with servo brakes, one passive rigid wheel and a controller. The caster with a servo brake is shown in Fig. 3. It has two rotary shaft as wheel shaft and pivot shaft as shown in Fig. 3. A servo brake is installed in only the wheel shaft of each caster. Two encoders are also installed on the wheel shaft and the pivot shaft of each caster for odometry.

The control performance of the robot depends on the characteristics of servo brakes. We used Powder Brake (MITSUBISHI Corp., ZKG-20YN, Maximum on-state Torque: 2.0[Nm]) as the servo brake. It provides high responsibility and good linearity on controlling the braking torque of wheels.

In passive moving system with casters, Peshkin et al. developed Cobot [2], in which its angle of the pivot shaft of the non-offset caster is only controlled by the servo motor. On the other hand, in our robot system, a servo brake is installed in the wheel shaft of each caster, not installed in the pivot shaft of each caster because it is an important advantage of casters that casters change the direction passively based on external force and moment. In this paper, we verify that the motion of the robot is controlled only the servo brake installed in the wheel shaft of each caster. As future works, we will develop a passive mobile robot with three or four casters with servo brakes which can move in all directions by extending the control method of caster with servo brake proposed in this paper.

III. Motion Control Algorithm

A. Kinematics of Mobile Robot with Casters

The direction of each caster changes based on motion of the robot, so that each component in Jacobian of the kinematics of mobile robot with casters is not constant and is a function consisting of the heading direction of each caster. It is greatly different from mobile robots with rigid wheels or omni-directional wheels. Therefore, we need to calculate each component in Jacobian by using the angular information of encoders installed on the pivot shafts in real time. The robot coordinate system is set as shown in Fig. 4 and Fig. 5. The kinematics between the motion vector of the robot

$\dot{\boldsymbol{q}}$ on the origin ${}^{r}o$ of the robot coordinate system and the angular velocity vector of casters $\boldsymbol{\omega}$ can be expressed as the following equation [7].

$$\dot{\boldsymbol{q}} = \boldsymbol{R}^{-1}\begin{bmatrix}\boldsymbol{J}_1 & \boldsymbol{J}_2\end{bmatrix}\boldsymbol{\omega} \tag{1}$$

where,

$$\dot{\boldsymbol{q}} = \begin{bmatrix}{}^{r}\dot{x} & {}^{r}\dot{y} & \dot{\alpha}\end{bmatrix}^T \tag{2}$$

$$\boldsymbol{\omega} = \begin{bmatrix}\omega_{w1} & \omega_{s1} & \omega_{w2} & \omega_{s2}\end{bmatrix}^T \tag{3}$$

$$\boldsymbol{J}_i = \frac{1}{2}\begin{bmatrix} r\cos\phi_i & -s\sin\phi_i \\ r\sin\phi_i & s\cos\phi_i \\ -r\sin(\theta_i-\phi_i)/L & -s\cos(\theta_i-\phi_i)/L \end{bmatrix} \tag{4}$$

$$\boldsymbol{R} = \begin{bmatrix} 1 & 0 & \frac{1}{2}\sum_{i=1}^{2} s\sin\phi_i \\ 0 & 1 & -\frac{1}{2}\sum_{i=1}^{2} s\cos\phi_i \\ 0 & \frac{1}{2L}\sum_{i=1}^{2}\cos\theta_i & 1-\frac{1}{2L}\sum_{i=1}^{2} s\cos(\theta_i-\phi_i) \end{bmatrix} \tag{5}$$

Jacobian $\boldsymbol{J}$ is expressed as the following equation.

$$\boldsymbol{J} = \boldsymbol{R}^{-1}\begin{bmatrix}\boldsymbol{J}_1 & \boldsymbol{J}_2\end{bmatrix} \tag{6}$$

Here, ω_{wi} and ω_{si} denotes the angular velocity of the wheel shaft and the pivot shaft, respectively. r denotes the radius of the wheel and s denotes the length of offset. ϕ_i denotes the angle of the pivot shaft. L denotes the distance between the origin ${}^{r}o$ and each pivot shaft, and θ_i denotes the angle between ${}^{r}x$-axis and $\overrightarrow{{}^{r}oc_i}$.

B. Characteristics of Servo Brake

The robot moves based on only the external force and moment applied to it, because it does not have any actuators such as servo motors. This is a very important feature in realizing safety actions. It is obvious that the characteristics of the brake system of wheel are complicated compared to a motor-wheel system. The characteristics of brake system depend on the wheel rotational direction. The sign of output torque of the wheel is decided by the direction of the wheel rotation and the magnitude of the torque is proportional to the input current of the brake. We have the following condition between the angular velocity of the wheel and the braking torque of a brake-wheel system.

$$\tau_b\omega_w \leq 0 \tag{7}$$

where τ_b is the brake torque generated by the servo brake and ω_w is the angular velocity of the wheel with a servo brake. This condition is the servo brake control constraint and indicates that one cannot have arbitrary torque from a servo brake. Therefore we need to consider the feasible brake torque τ_b during motion control of a robot [6].

C. Motion Control of Passive Mobile Robot

Under the assumption that the center of mass m of the robot is the position of the rigid wheel, as shown in Fig. 4, the damping coefficient is defined as D, the inertial moment and the damping coefficient around the center of mass are defined as J and D_θ, respectively, and the velocity and the acceleration on the position of the rigid wheel are defined as $\dot{\boldsymbol{q}}_w$ and $\ddot{\boldsymbol{q}}_w$, respectively. This robot does not consider the velocity, the acceleration and force of ${}^{r}y$ axial direction because this robot has a rigid wheel and could not move to ${}^{r}y$ axial direction according to the non-holonomic constraint. Therefore, a position and an orientation of the rigid wheel is difined with respect to the $\sum_r$ as $\boldsymbol{q}_w = \begin{bmatrix}{}^{r}x_w & \alpha\end{bmatrix}^T$. The robot's dynamics, based on the force/moment $\boldsymbol{F}_h = \begin{bmatrix}f_h & n_h\end{bmatrix}^T$ applied by a human and the braking force/moment $\boldsymbol{F}_b = \begin{bmatrix}f_b & n_b\end{bmatrix}^T$ generated by the servo brakes, is expressed as follows:

$$\boldsymbol{M}\ \ddot{\boldsymbol{q}}_w + \boldsymbol{D}\ \dot{\boldsymbol{q}}_w = \boldsymbol{F}_h + \boldsymbol{F}_b \tag{8}$$

where,

$$\boldsymbol{M} = \begin{bmatrix} m & 0 \\ 0 & J \end{bmatrix}, \boldsymbol{D} = \begin{bmatrix} D & 0 \\ 0 & D_\theta \end{bmatrix},$$
$$\boldsymbol{q}_w = \begin{bmatrix} {}^{r}x_w \\ \alpha \end{bmatrix}, \boldsymbol{F}_h = \begin{bmatrix} f_h \\ n_h \end{bmatrix}, \boldsymbol{F}_b = \begin{bmatrix} f_b \\ n_b \end{bmatrix} \tag{9}$$

where $\boldsymbol{M} \in \boldsymbol{R}^{2\times2}$ is the inertia matrix, and $\boldsymbol{D} \in \boldsymbol{R}^{2\times2}$ is the damping matrix. In this research, the braking force/moment $\boldsymbol{F}_b = \begin{bmatrix}f_b & n_b\end{bmatrix}^T$ generated by the brakes is controlled for realizing an arbitrary motion of the robot and, as shown in Fig. 4, we derive the brake torque $\boldsymbol{\tau}_b = \begin{bmatrix}\tau_{b1} & \tau_{b2}\end{bmatrix}$ for each wheel as follows:

$$\boldsymbol{\tau}_b = \begin{bmatrix}\tau_{b1} \\ \tau_{b2}\end{bmatrix} = \boldsymbol{A}^{-1}\begin{bmatrix}f_b \\ n_b\end{bmatrix} \tag{10}$$

where,

$$\boldsymbol{A} = \frac{1}{r}\begin{bmatrix} \cos\phi_1 & \cos\phi_2 \\ -B\sin\phi_1 - L\cos\phi_1 & -B\sin\phi_2 + L\cos\phi_2 \end{bmatrix} \tag{11}$$

where B is the distance between the origin ${}^{r}o$ of the robot coordinate system and the position of the rigid wheel.

Now, we consider the case that we can not derive the inverse matrix of $\boldsymbol{A}$. In this case, the determinant of matrix $det\boldsymbol{A}$ is derived as

$$det\boldsymbol{A} = \frac{1}{r^2}\{B\sin(\phi_1-\phi_2) + \frac{L}{2}\cos\phi_1\cos\phi_2\} = 0 \tag{12}$$

where eq.(12) has equality if

$$\phi_1 = 90^\circ\ or\ 270^\circ\ and\ \ \phi_2 = 90^\circ\ or\ 270^\circ \tag{13}$$

This is the singular position of the robot as shown in Fig. 6. However, in this paper, we do not control the system in the case expressed in eq.(13), because this case is very short period and the casters change the direction immediately based on external force and moment. We will consider how to control the robot at the singular point as future works.

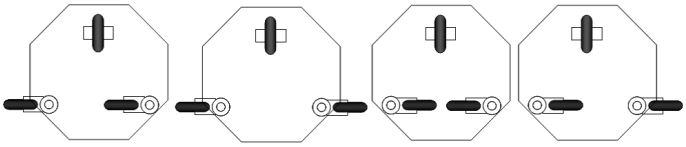

Fig. 6. Singular Orientations of Casters

TABLE I
MOTION TYPE BASED ON BRAKE CONDITIONS OF THE ROBOT

	Sign of Angular Wheel Velocity			
Caster Left	+	+	-	-
Caster Right	+	-	+	-
Motion Type	1	2	3	4

D. Feasible Braking Force/Moment

As mentioned in the previous section B, we need to consider that the servo brake applies a torque to the wheel according to the sign of the rotational direction of the wheel, which influences the feasible braking force and moment applied to the robot. The derivation of the feasible braking force and moment based on the servo brake condition is very important for control of the passive robot system.

Here, we consider the relationship between the direction of casters and the feasible braking force and moment. First, we classify the motion of the robot into 4 different cases based on the signs of the angular velocities of the wheels of two casters as shown in Tab.I. The motion types of the robot can be classified by 9 different cases exactly, if we consider that the velocity of a wheel equal to zero. However, in this paper, we only consider that each wheel rotates with a velocity for the simplicity of the discussion. In each motion type, the servo brake control constraint in eq.(7) should be considered in the derivation of the feasible braking torques. The feasible braking force and moment are generated by using these feasible braking torques and the following equation.

$$\boldsymbol{F}_b = \boldsymbol{A}\boldsymbol{\tau}_b \tag{14}$$

We explain how to derive the feasible region of braking force and moment theoretically in [6]. The example of the feasible braking force and moment set in the case of Motion-Type 1 is shown in Fig. 7. In Fig. 7 the horizontal axis expresses the feasible braking force ${}^r f_x$ along ${}^r x$ and the vertical axis expresses the feasible moment ${}^r n_z$. As you can see, the feasible braking force and moment are limited.

Next, we explain the feasible braking force and moment based on the servo brake condition [6]. We define $\boldsymbol{F}_d$ and $\boldsymbol{F}_w$ as the desired force/moment and the feasible braking force/moment, respectively. During controlling a mobile robot, the desired force/moment $\boldsymbol{F}_d$ should be generated in real time which are determined by the control law applied to the system such as motion control for path tracking, obstacle collision avoidance, impedance control, etc. For an active type robot using servo motors, we just simply command to servo motors of the robot to generate torques for realizing

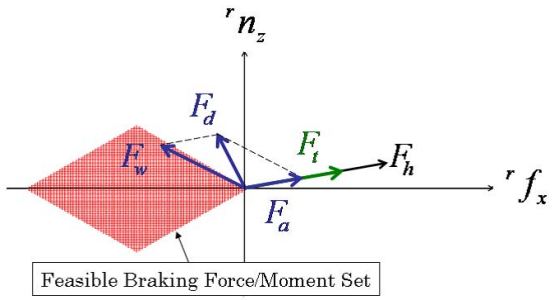

Fig. 7. Control of Robot Based on Feasible Braking Force and Moment

this desired force/moment $\boldsymbol{F}_d$. However, in the control of a passive robot system, the feasible force and moment are always depending on the current motion of the system.

If the desired force/moment $\boldsymbol{F}_d$ is within the feasible force and moment set in the current motion of the robot which is determined by the sign of the angular velocities of the wheels explained above, we can command the brake torques of the wheels directly as $\boldsymbol{F}_w = \boldsymbol{F}_d$. On the other hand, of course, many cases exist that the desired force/moment $\boldsymbol{F}_d$ is located out of the feasible set of the force and moment, and cannot be generated by servo brakes. One typical example is that a passive robot cannot generate force or moment for accelerating the motion of the object by itself.

The system considered here is that a human operator is pushing or pulling the robot and from eq.(8) the system dynamics can be rewritten as follows:

$$\boldsymbol{M}\ \ddot{\boldsymbol{q}}_w + \boldsymbol{D}\ \dot{\boldsymbol{q}}_w = \boldsymbol{F}_h + \boldsymbol{F}_w \tag{15}$$

where the force/moment $\boldsymbol{F}_h$ applied by the human could be divided into two elements. One is the driving force/moment $\boldsymbol{F}_t$ utilized for moving the robot along the pushing or pulling direction of the human, and the other is the assistive force/moment $\boldsymbol{F}_a$ for realizing the several functions such as path tracking. This relationship is illustrated by the following equation.

$$\boldsymbol{F}_h = \boldsymbol{F}_t + \boldsymbol{F}_a \tag{16}$$

We discuss a motion control algorithm of the robot for realizing the several functions. The dynamics of the robot are expressed by eq.(16), and we consider the apparent dynamics of the robot expressed as follows:

$$\boldsymbol{M}\ \ddot{\boldsymbol{q}}_w + \boldsymbol{D}\ \dot{\boldsymbol{q}}_w = \boldsymbol{F}_t + \boldsymbol{F}_d \tag{17}$$

This equation means that the robot is moved based on the driving force/moment $\boldsymbol{F}_t$ and the desired force/moment $\boldsymbol{F}_d$ for realizing several functions.

From eq.(15) - eq.(17), we derive the following equation with respect to the braking force/moment $\boldsymbol{F}_w$.

$$\boldsymbol{F}_w = \boldsymbol{F}_d - \boldsymbol{F}_a \tag{18}$$

If we can specify the feasible brake force/moment $\boldsymbol{F}_w$ based on the above equation, the apparent dynamics of the robot expressed by eq.(17) is realized. In other words, eq.(18)

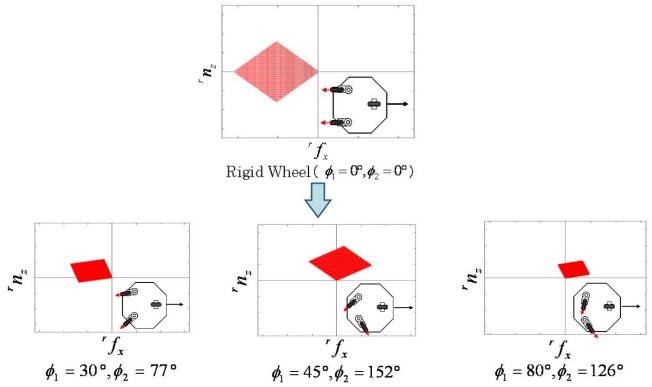

Fig. 8. Direction of Casters and Feasible Braking Force and Moment

means that the desired force/moment $\boldsymbol{F}_d$ is generated by the composition of the feasible braking force/moment $\boldsymbol{F}_w$ and the assistive force/moment $\boldsymbol{F}_a$ which is a part of the force/moment applied by the human as shown in Fig. 7 when $\boldsymbol{F}_d$ is out of the feasible braking force/moment set. From Fig. 7, you can see that we need to generate torques for realizing the braking force and moment $\boldsymbol{F}_w$ within the feasible braking force and moment set.

However, in this robot system with casters, since the braking force/moment $\boldsymbol{F}_b = \begin{bmatrix} f_b & n_b \end{bmatrix}^T$ is a function of ϕ_i (the direction of casters) in eq.(14), the set of feasible braking force and moment changes based on the direction of casters as the example shown in Fig. 8. Different from the robot with rigid wheels or omni-directional wheels, like RT Walker or PRP, we need to consider not only the direction of the wheel rotation but also the direction of casters during controlling the robot. One example of the relationship between $\boldsymbol{F}_w$ and the set of the feasible force and moment in the path tracking function is shown in Fig. 9. In the case of Fig. 9(a), the feasible braking force and moment $\boldsymbol{F}_w$ is located within the set of the feasible force and moment and the system can generate the desired force and moment $\boldsymbol{F}_d$. On the other hand, in the case of Fig. 9(b), the desired force and moment $\boldsymbol{F}_d$ is within the feasible force and moment set, so that the system can generate the desired force and moment as $\boldsymbol{F}_w = \boldsymbol{F}_d$. As above, we need to consider the current motion of the system which includes both the sign of the angular velocities of wheels and the direction of casters to generate the feasible braking force and moment properly.

IV. Experiment

In this paper, we conducted two experiments for illustrating the validity of the proposed passive robot system and its control algorithm. One is the experiment of the path tracking function and the other is the collision avoidance function. In both experiments, we consider that a human operator applies a force to the robot by pushing or pulling the robot.

A. Path Tracking Control

For illustrating the validity of this passive robot, we experimented the path tracking function with this robot. In

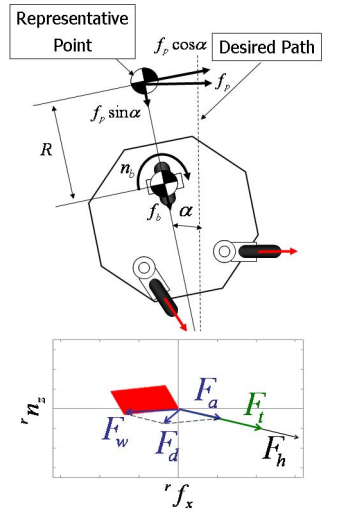

(a)Example 1

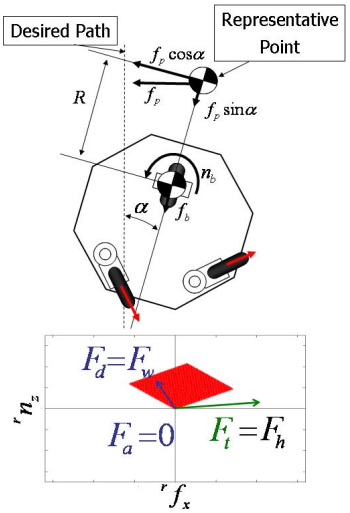

(b)Example 2

Fig. 9. Relationship between $\boldsymbol{F}_w$ and Feasible Braking Force and Moment

this experiment, a human applies a force along the x-axis of the robot coordinate system by pushing as shown in Fig. 10 and the robot is controlled based on the desired braking force f_p along y-axis of the global coordinate system to follow a line which is designed as follows:

$$ {}^o y_{des} = b \cos \frac{2\pi\, {}^o x_{cur}}{a} - b \tag{19} $$

$$ {}^o \dot{y}_{des} = \frac{2\pi b\, {}^o \dot{x}_{cur}}{a} \sin \frac{2\pi\, {}^o x_{cur}}{a} \tag{20} $$

where ${}^o y_{des}$ and ${}^o \dot{y}_{des}$ express the desired position and the velocity of the robot along y-axis of the global coordinate system, and ${}^o x_{cur}$ and ${}^o \dot{x}_{cur}$ are the real position and the velocity along x-axis of the global coordinate system. Here, $b = 4.0[m]$, $a = 0.25[m]$. From these equations, we can design the desired braking force f_p as following equation

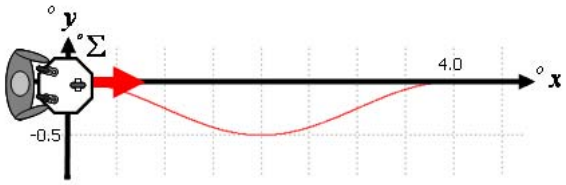

Fig. 10. Experimental Method of Path Tracking Function

for the path tracking control [6].

$$f_p = -K_p({}^o y - {}^o y_{des}) - K_d({}^o\dot{y} - {}^o\dot{y}_{des}) \quad (21)$$

$$f_b = f_p \sin\alpha \quad (22)$$

$$n_b = R f_p \cos\alpha \quad (23)$$

where f_p is applied to the representative point on the front of the robot as shown in Fig. 9, ${}^o y$ and ${}^o\dot{y}$ are the real position and the real velocity along y-axis of the global coordinate system, K_p and K_d are the proportional and derivative gains, and R is the distance between the position of the rigid wheel and the representative point on the front of the robot, respectively.

Experimental results are illustrated in Fig. 11. Fig. 11(a) expresses the position and the orientation of the robot on xy-plane, Fig. 11(b),(c) express the position and the velocity of the robot along ${}^o y$ direction with respect to the time. Fig. 11(d) expresses the orientation of the robot with respect to the time, and Fig. 11(e) expresses the angle of each pivot shaft. Fig. 11(f),(g) are braking force and moment applied to the robot with respect to the time. From Fig. 11, the path tracking function is successfully achieved.

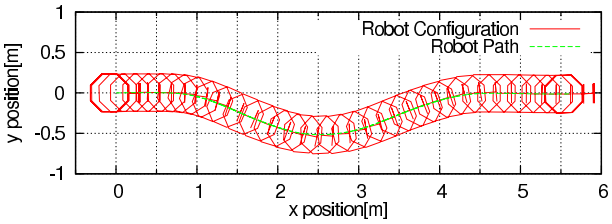

(a) Path of Robot

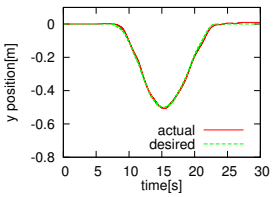

(b) Position ${}^o y$

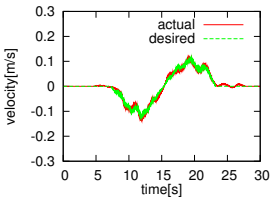

(c) Velocity ${}^o\dot{y}$

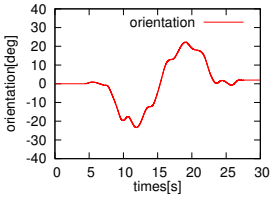

(d) Orientation ${}^o\alpha$

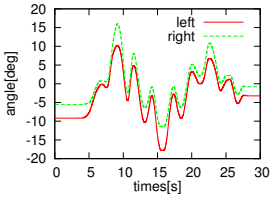

(e) Angle of each Pivot Shaft

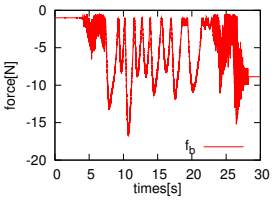

(f) Control Input f_b

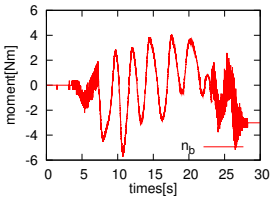

(g) Control Input n_b

Fig. 11. Experimental Results of Path Tracking Function

B. Collision Avoidance Control

In this section, we experimented the collision avoidance control. In this experiment, we derive the virtual force and moment generated based on environmental information to avoid collision with obstacles. We use a method called artificial potential field, proposed by Khatib [8], which is generally used in research on robot collision avoidance. We designed the artificial potential field $\boldsymbol{U}(\boldsymbol{q}_R)$ based on the positions of obstacles as follows [5]:

$$\boldsymbol{U}(\boldsymbol{q}_R) = \begin{cases} k\left(1 + \cos\dfrac{\pi}{\rho_o}\rho(\boldsymbol{q}_R)\right) & (\rho(\boldsymbol{q}_R) \le \rho_o) \\ 0 & (\rho(\boldsymbol{q}_R) > \rho_o) \end{cases} \quad (24)$$

where $\boldsymbol{q}_R = [{}^o x_R, {}^o y_R, \alpha]$ is the position and orientation of the representative point on the front of the robot, as shown in Fig. 12, k is the positive constant gain, $\rho(\boldsymbol{q}_R)$ is the shortest distance from $\boldsymbol{q}_R$ to an obstacle, and ρ_o is the limit distance of the potential field influence. From eq.(19), $\boldsymbol{U}(\boldsymbol{q}_R)$ is larger than zero and increases when the robot is close to obstacles. On the other hand, when $\rho(\boldsymbol{q}_R)$ is larger than ρ_o, $\boldsymbol{U}(\boldsymbol{q}_R)$ is equal to zero.

From eq.(19), we generate the virtual force and moment $\boldsymbol{F}(\boldsymbol{q}_R)$ applied to the position of the rigid wheel as follows:

$$\boldsymbol{F}(\boldsymbol{q}_R) = -\nabla \boldsymbol{U} \quad (25)$$

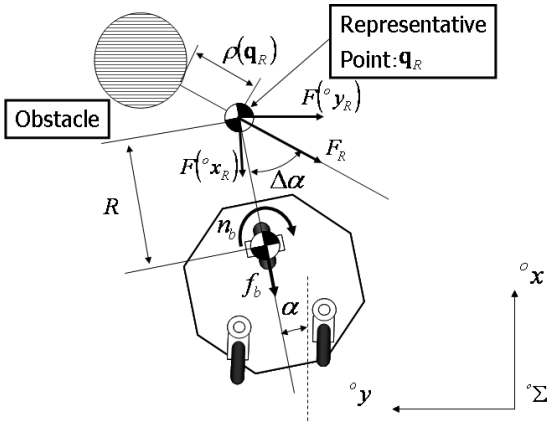

Fig. 12. Relationship between Robot and Obstacle

where $\nabla \boldsymbol{U}$ is the gradient vector of $\boldsymbol{U}$ with respect to $\boldsymbol{q}_R$. From this equation, we can derive the virtual force $\boldsymbol{F}(\boldsymbol{q}_R)$ applied to the position of the rigid wheel as follows:

$$\boldsymbol{F}(\boldsymbol{q}_R) = \begin{cases} \dfrac{k\pi}{\rho_o}\rho(\boldsymbol{q}_R)\sin\dfrac{\pi}{\rho_o}\rho(\boldsymbol{q}_R) & (\rho(\boldsymbol{q}_R) \le \rho_o) \\ 0 & (\rho(\boldsymbol{q}_R) > \rho_o) \end{cases} \quad (26)$$

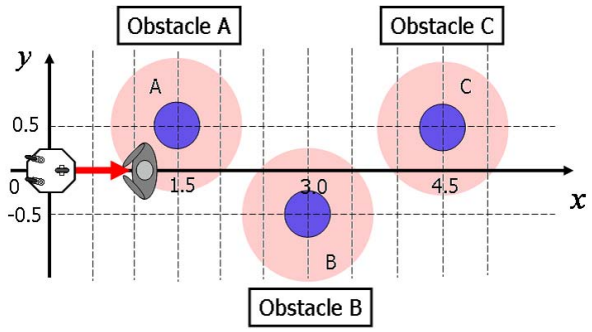

Fig. 13. Experimental Method of Collision Avoidance

From eq.(21), we derive the virtual force and moment $\boldsymbol{F}_r = \begin{bmatrix} f_r & n_r \end{bmatrix}^T$ applied to the position of the rigid wheel and the braking force and moment $\boldsymbol{F}_b = \begin{bmatrix} f_b & n_b \end{bmatrix}^T$ as follows:

$$f_b = f_r = -F_R \cos \Delta\alpha \tag{27}$$

$$n_b = n_r = RF_R \sin \Delta\alpha \tag{28}$$

where R is the distance between the position of the rigid wheel and the representative point, and F_R and $\Delta\alpha$ are expressed as

$$F_R = \sqrt{F^2({}^o x_R) + F^2({}^o y_R)} \tag{29}$$

$$\Delta\alpha = \alpha - \tan^{-1} \frac{F({}^o x_R)}{F({}^o y_R)} \tag{30}$$

In this experiment, a human applies a force along the x-axis of the robot coordinate system by pulling as shown in Fig. 13. Three obstacles are placed at $A(1.5, 0.5)$, $B(3.0, -0.5)$, $C(4.5, 0.5)$ on xy-plane as shown in Fig. 13 and we specify the positions of three obstacles to the robot in advance. We generate an artificial potential field by specifying the following parameters: $\rho_o = 0.8$, $R = 0.3$, $k = 8.0$.

Experimental results are illustrated in Fig. 14. Fig. 14(a) expresses the path of the robot with respect to xy-plane when the human applies a force by pulling. The motion of the experiment is shown in Fig. 14(b). From Fig. 14, you can see that the robot avoids collision with obstacles and collision avoidance motion is realized by controlling the braking force of casters appropriately.

V. Conclusion

In this paper, we introduced a new passive-type object handling robot consisting of casters with servo brakes based on a concept of passive robotics. This robot consists of two casters with servo brakes and one passive rigid wheel. We proposed the fundamental motion control algorithm of this robot system. The analysis of the feasible braking force and moment set, which depends on the motion of system and the direction of casters, are provided. The proposed motion control algorithm is implemented to the robot actually, and experimental results on the path tracking motion control and

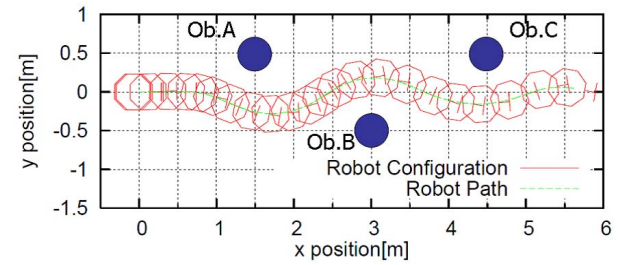

(a)Path of Robot

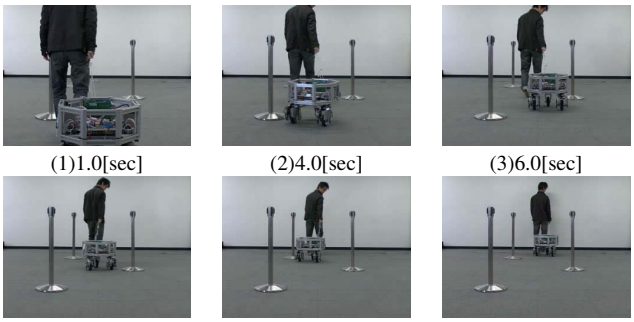

(1)1.0[sec] (2)4.0[sec] (3)6.0[sec]

(4)7.5[sec] (5)9.0[sec] (6)12.0[sec]

(b)Motion of Experiment for Collision Avoidance

Fig. 14. Experimental Results of Collision Avoidance

the collision avoidance motion control illustrated the validity of the proposed system and algorithm.

As future works, based on the fundamental motion control algorithm, we will develop a passive mobile robot with three or four casters with servo brakes which can move in all directions. In addition, we will consider the singularity and the redundancy of the robot with many casters, and focus on the improvement of the maneuverability of the moving bases with casters used widely in the real world.

References

[1] A. Goswami, M. A. Peshkin, J. Colgate, "Passive robotics: an exploration of mechanical computation", Proc. of the IEEE International Conference on Robotics and Automation, pp.279-284, 1990.

[2] M. A. Peshkin, J. E. Colgate, W. Wannasuphoprasit, C. A. Moore, R. B. Gillespie, P.Akella, "Cobot Architecture", IEEE Transactions on Robotics and Automation, Vol.17, No.4, pp.377-390, 2001.

[3] G. Wasson, P. Sheth, M. Alwan, K. Granata, A. Ledoux, C. Huang, "User Intent in a Shared Control Framework for Pedestrian Mobility Aids", Proc. of the 2003 IEEE/RSJ International Conference on Intelligent Robots and Systems, Vol.3, pp.2962-2967, 2003.

[4] A. J. Rentschler, R. A. Cooper, B. Blaschm M. L. Boninger, "Intelligent walkers for the elderly : Performance and safety testing of VA-PAMAID robotic walker", Journal of Rehabilitation Research and Development, Vol.40, No.5, pp.423-432, 2003.

[5] Y. Hirata, A. Hara, K. Kosuge, "Motion Control of Passive Intelligent Walker Using Servo Brakes", Proc. of the IEEE Transactions on Robotics and Automation, Vol.23, No.5, pp.981-990, 2007.

[6] Y. Hirata, Z. Wang, K. Fukaya, K. Kosuge, "Transporting an Object by a Passive Mobile Robot with Servo Brakes in Cooperation with a Human", Advanced Robotics, Vol.23, No.4, pp.387-404, 2009.

[7] M. Wada, "Modeling and Control of Omnidirectional Mobile Robots with Active Casters", Journal of the Robotics Society of Japan Vol.25 No.7, pp.1100-1107, 2007 (in Japanese).

[8] O. Khatib, "Real-Time Obstacle Avoidance for Manipulators and Mobile Robots", International Journal of Robotics Research, pp.90-98, 1986.